frontiers | Frontiers in Mechanical Engineering

TYPE Original Research
PUBLISHED 02 January 2026
DOI 10.3389/fmech.2025.1710472

OPEN ACCESS

EDITED BY
Chengxi Zhang,
Jiangnan University, China

REVIEWED BY
Yu Yan,
Sun Yat-sen University, China
Hui Huang,
Huaqiao University, China
Lanhao Zhao,
Beijing University of Technology, China

*CORRESPONDENCE
Feifei Zhao,
zff111030@163.com

RECEIVED 22 September 2025
REVISED 07 December 2025
ACCEPTED 08 December 2025
PUBLISHED 02 January 2026

CITATION
Zhao F (2026) Design of constant force polishing device for castings based on kinematic analysis.
Front. Mech. Eng. 11:1710472.
doi: 10.3389/fmech.2025.1710472

Design of constant force polishing device for castings based on kinematic analysis

Feifei Zhao*

School of Intelligent Manufacturing, Zibo Polytechnic University, Zibo, China

Introduction: In response to the problem of insufficient stability in force control of existing polishing equipment, this study aims to develop a casting constant force polishing device based on kinematic analysis to meet the high-precision and high-efficiency requirements of surface machining of large castings.
Methods: Starting from the casting processing technology, combined with mechanical principles and optimization design methods, the overall structural design and optimization of the polishing device are completed. At the same time, a kinematic model is established and a control system based on programmable logic controller is constructed.
Results: The results of motion simulation and adaptability verification show that the polishing device exhibits good adaptability and stability under different surface characteristics of castings, and the trajectory accuracy can reach up to 90%. The average polishing force can quickly stabilize under different characteristics, and the average polishing force of planar features remains stable between 490 N and 500 N with minimal fluctuations. The improved proportional-integral-derivative control strategy significantly improves control accuracy and response speed, with a minimum root mean square error value of 0.08 and an error recovery time of only 4.0 s.
Discussion: The research designed constant force polishing device for castings not only improves the surface machining quality of castings, but also provides an efficient and stable solution for automated polishing of large castings, which has important industrial application value.

KEYWORDS

constant force polishing device for castings, kinematics, PID, PLC control system, structural optimization

1 Introduction

In modern industrial manufacturing, surface machining of castings is one of the key links to ensure product quality. With the continuous development of industrial technology, the requirements for the surface quality of castings are becoming increasingly high, and traditional polishing processes are no longer able to satisfy the production needs of high precision and high efficiency. Due to their large size and complex shape, large castings are more difficult to process on the surface, especially during the polishing process where a constant polishing force needs to be maintained to avoid surface quality degradation caused by force fluctuations (Trojnacki and Dabek, 2024; Song et al., 2023a). In the field of mechanical design and control, kinematic analysis is the fundamental theory for studying the motion characteristics of mechanical systems, and is widely used in the design and optimization of robots and automation equipment. Through kinematic models, the pose changes of mechanical systems can be accurately described, providing theoretical support

for achieving high-precision control (Pacioni et al., 2024; Lyu and Purwar, 2025). Programmable Logic Controller (PLC) has become the core component of industrial automation control systems because of its high reliability, ease of programming, and powerful processing capabilities. Proportional-Integral-Derivative Control (PID), as a classic feedback control strategy, is broadly utilized in the field of industrial automation due to its simplicity, ease of implementation, and significant control effects. With the development of intelligent manufacturing technology, combining kinematic analysis, PID control, and PLC technology has become an important means to solve complex industrial automation problems (Yitao et al., 2024; Xu et al., 2024).

In the field of industrial automation equipment design and complex system control, structural optimization and precise control for different application scenarios have always been the core direction of research. Relevant technological achievements provide important references for the design of Constant Force Polishing Devices (CFPDs) for castings. Regarding the design and performance evaluation of lower limb rehabilitation devices, Sun et al. proposed a design scheme for knee ankle orthotics, and established its dynamic model based on the thermodynamic model of shape memory alloy. The dynamic response adjustment accuracy of the knee joint under different working states was optimized through PID. The findings denoted that the max displacement of the shape memory alloy spring actuator was 54.36 mm, the max restoring force during the phase transition process was 4.14 newtons, and the max rotation angle was 43.18° (Sun et al., 2023). In response to the problem that traditional rigid robot modeling and control theory is not applicable to soft robots, Emet et al. simplified the complex model of ultra redundant software robots through segmented constant curvature approximation, and combined it with PLC control system to make it suitable for real-time applications. The research results indicated that this method could be effectively applied to the modeling of soft robots and validated in the soft arm teleoperation of biomimetic octopus robots, providing a new solution for underwater operations (Emet et al., 2024). For the issue of existing ankle rehabilitation robots being unable to fully adapt to the complex movements of the human ankle joint and having poor human-machine compatibility, Song et al. developed an equivalent serial mechanism model that closely matches the actual skeletal structure of the human ankle joint. This model was programmed using PLC to ensure precise execution. The research results indicated that based on the mapping relationship and equivalent model of motion characteristics and physiological structure, a parallel ankle joint rehabilitation robot configuration was successfully designed, and the rehabilitation effect was verified through human-machine coupling rehabilitation simulation model (Song et al., 2023b). Simas et al. proposed a novel parallel robot to address the problems of alignment difficulties and limited workspace in traditional parallel robots. The robot compensated for the possible misalignment of the driving sliding pair by introducing passive joints in the support chain, and improved the accuracy of the support chain motion with PID control algorithm. The research findings indicated that the forward and reverse position analysis of the new parallel robot had simple closed form solutions, and there were significant singular regions in its workspace (Simas et al., 2022).

In summary, existing research has not established a constant force control model applicable to the complex surface characteristics of castings, nor has it proposed a solution to the problem of surface quality degradation caused by force fluctuations during the polishing. Meanwhile, the special requirements of polishing equipment for high stiffness, high dynamic response, and real-time adjustment of force feedback have not been fully considered. The purpose of the research is to design a CFPD for castings based on kinematic analysis, to solve the problem of insufficient force control stability of existing polishing equipment and meet the high-precision and high-efficiency requirements for surface processing of large castings. The core of this method lies in optimizing the structural design of the grinding device, establishing an accurate kinematic model, and combining advanced control strategies to realize precise control of polishing force and adaptive adjustment of different casting surface characteristics.

The innovation points of this research are mainly reflected in three aspects: Firstly, an overall design scheme of the constant force grinding device for castings based on kinematic analysis is proposed. Through the topology optimization method, the weight of the parallel platform structure is reduced and the stiffness is strengthened. While meeting the strength requirements, the dynamic response speed is improved. Moreover, the force sensor is innovatively integrated between the parallel platform and the end effector to achieve real-time feedback of the grinding force and pose linkage adjustment. Different from the design logic of traditional grinding devices that only focus on position control; Secondly, a simplified and actual working condition parallel platform kinematic model is constructed. Based on the assumption that the rotation of the moving plate is around a fixed axis and the translation is mainly in the vertical direction, the mapping relationship between the extension and contraction of the side chain and the movement of the moving plate is precisely described through the uniform transformation matrix and the Jacobian matrix, which not only reduces the computational complexity to meet the real-time control requirements It also reserves expansion space for the subsequent optimization of multi-degree-of-freedom models under complex working conditions. Thirdly, an improved PID control strategy integrating fuzzy logic and adaptive mechanism was developed. By constructing a fuzzy rule base containing 49 rules to dynamically correct PID parameters and combining rolling time-domain error feedback to achieve adaptive update of parameter base values, the problems of low control accuracy and response lag of traditional PID under nonlinear disturbances during the grinding process were solved. Provide a technical solution that combines precision and adaptability for the automatic constant force grinding of large castings.

2 Methodology

The study first designs and optimizes the overall structure of the polishing device for the machining requirements of castings, ensuring that it meets the requirements of high precision, high efficiency, and force control stability. Subsequently, a kinematic model is built grounded on the geometric and motion characteristics of the parallel platform, providing a theoretical basis for subsequent control strategy design. Finally, a control system with PLC as the

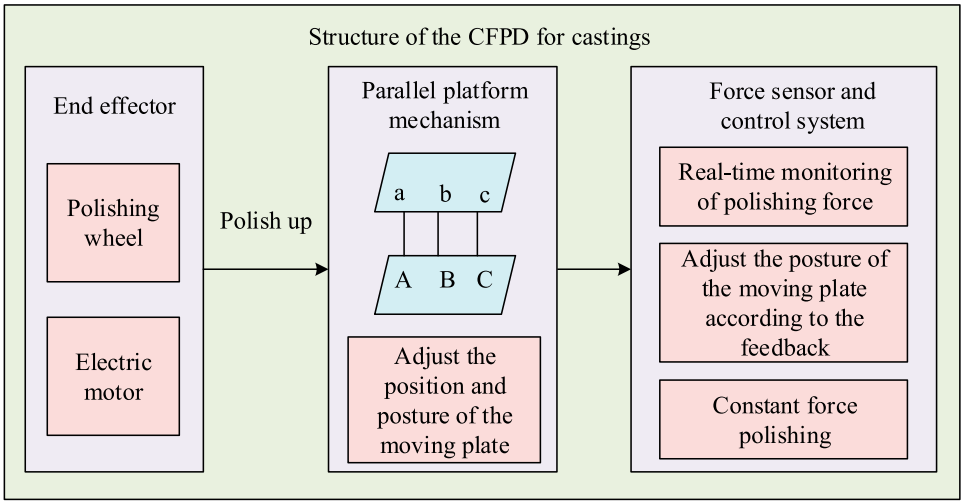

FIGURE 1
Structural design of constant force polishing device for castings.

core is designed, adopting an improved PID control strategy to achieve automation and precise control of the polishing process.

2.1 Structural design and optimization of constant force polishing device for castings

Starting from the machining process requirements of castings, combined with mechanical principles and optimization design methods, the overall structural design and optimization of the polishing device have been completed. The design of the constant force polishing device (CFPD) for castings needs to ensure that the force applied to the surface of the casting during the polishing process remains constant, avoiding a decrease in the surface quality of the casting due to force fluctuations. It must be adaptable to castings of different sizes and shapes, as well as different surface characteristics of castings. It should be easy to install and maintain, while ensuring sufficient rigidity and strength to withstand the loads during the grinding process. While meeting strength and stiffness requirements, the weight of the device should be minimized as much as possible to improve its dynamic response speed (Yang et al., 2023; Buonocore et al., 2023). The structural design of the CFPD for castings is shown in Figure 1.

In Figure 1, the end effector is composed of a grinding wheel and a motor, responsible for directly contacting the casting and completing the grinding task, requiring high speed, high precision, and sufficient torque. The parallel platform mechanism contains a fixed plate, a moving plate, and three branch chains. Its function is to adjust the position and posture of the moving plate to adapt to changes in the casting surface. It must therefore be highly stiff and precise, and have good dynamic performance. The force sensor and control system consist of a force sensor and a controller, which are used to monitor the polishing force in real time and adjust the position of the moving plate based on feedback to achieve constant force polishing, requiring high precision, fast response, and stability. The selection of grinding wheel needs to be optimized according to the casting material and grinding requirements. The relationship between the linear velocity of the grinding wheel and the motor speed is shown in Equation 1.

$$v = \pi D n \tag{1}$$

In Equation 1, D means the diameter of the grinding wheel in meters, v means the linear velocity of the grinding wheel in meters per second, and n is the motor speed in revolutions per minute. According to the polishing requirements, the linear speed of the grinding wheel needs to reach a certain value to ensure the polishing effect. The kinematic model of a parallel platform can be described by a homogeneous transformation matrix (Wei, 2022; Song et al., 2024). The pose relationship of the moving coordinate system (MCS) relative to the fixed coordinate system (FCS) is shown in Equation 2.

$$T = \begin{bmatrix} x_i & y_i & z_i & x_c \\ x_j & y_j & z_j & y_c \\ x_k & y_k & z_k & z_c \\ 0 & 0 & 0 & 1 \end{bmatrix} \tag{2}$$

In Equation 2, T is a homogeneous matrix, and x_i, y_i, and z_i represent the coordinate differences between the X-axis of the MCS and the FCS; x_j, y_j, and z_j indicate the coordinate differences between the Y-axis of the MCS and the FCS; x_k, y_k and z_k represent the coordinate differences between the Z-axis of the MCS and the FCS; x_c, y_c, and z_c represent the spatial positions of the origin of the MCS in a FCS. The force sensor is installed between the parallel platform and the end effector for real-time monitoring of force information during the polishing process, and feeds back the data to the control system. The control system adjusts the feed rate and position of the polishing tool in real time, using feedback from the force sensor, to achieve constant-force polishing (Ramanababu and Ramji, 2024; Wei et al., 2024). The feedback control law of the control system is denoted in Equation 3.

$$u(t) = K_p(F_d - F(t)) + K_i \int_0^t (F_d - F(\tau))\mathrm{d}\tau + K_d \frac{\mathrm{d}}{\mathrm{dt}}(F_d - F(t)) \tag{3}$$

TABLE 1 Structural parameters of constant force polishing device for castings.

Parameter name	Parameter description	Unit	Typical value
Moving plate size	The physical dimensions of the moving plate	mm	500 × 300
Static plate size	The physical dimensions of the static plate	mm	600 × 400
The number of branch chains	The number of side chains connecting the moving plate and the stationary plate	a	3
Side chain length	The length of the side chain in its initial state	mm	Seven hundred
Drive type	The type of driver used to drive the expansion and contraction of side chains	Type	Electric
Force sensor range	The maximum force value that the force sensor can measure	N	500
Controller type	The types of control systems	Type	PLC
Grinding speed	The moving speed of the grinding head on the surface of the casting	m/min	5–10
Grinding accuracy	The roughness of the surface of the casting after grinding	um	1.6

In Equation 3, F is the force measured by the force sensor, $u(t)$ denotes the control input, F_d is the expected polishing force, and K_p, K_i, and K_d indicate the proportional, integral, and derivative control parameters, respectively. To further improve the performance of the parallel platform mechanism, structural optimization is studied. The purpose of optimization is to minimize the weight of the platform and improve the dynamic performance of the device while meeting the requirements of strength and stiffness. The study adopts topology optimization methods to adjust material distribution, remove unnecessary materials, while ensuring the strength and stiffness of the structure. The optimized structure significantly reduces weight and improves dynamic performance while meeting design requirements. After optimization, the structural parameters of the casting CFPD designed for research are denoted in Table 1.

Table 1 denotes the key structural parameters of the CFPD for castings, including the dimensions of the moving plate and the stationary plate, which are 500 × 300 mm and 600 × 400 mm respectively, as well as three branch chains connecting them. The initial length of the branch is 700 mm, driven by the corresponding type of driver, using an electric driver. The range of the force sensor reaches 500 Newtons, and the controller type is PLC. The grinding speed range is 5–10 m per minute and the grinding accuracy requirement is 1.6Ra, which together ensure that the grinding device can be precisely adjusted and operate efficiently according to the specific needs of the casting. The optimization objective function takes minimizing the structural weight as its core and sets key constraints at the same time. The natural frequency shall not be lower than 200 Hz and the maximum stress shall not exceed the allowable stress of the material used. The design area focuses on the high-stress and high-deformation sensitive parts of the parallel platform, including the web areas of the moving plate and the static plate, and the connection joints between the branch chain and the platform. The material selected is 6061-T6 aluminum alloy, which is commonly used in industrial automation equipment. It has an elastic modulus of 69 GPa and a Poisson's ratio of 0.33, taking into account both lightweight and structural strength requirements. The grid division adopts tetra4 elements, with the minimum element size set at 5 mm, focusing on ensuring the calculation accuracy of stress concentration areas such as branch chain joints. The volume fraction constraint is set to no more than 0.6, meaning that the weight of the optimized structure is reduced by no more than 40% compared to the initial model. While reducing the weight, excessive loss of stiffness is avoided (Scavalla et al., 2023; Wang et al., 2023).

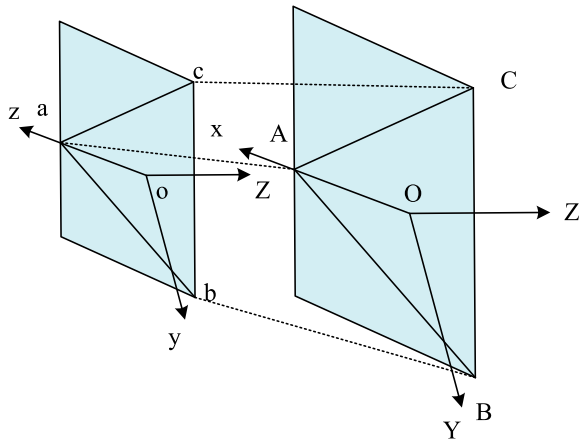

FIGURE 2
Parallel platform coordinate system.

2.2 Establishment of kinematic model for constant force polishing device for castings

After completing the structural design and optimization of the CFPD for castings, the research further focuses on the kinematic characteristics analysis of the device. The kinematic model of the CFPD for castings is established ground on the structure and motion characteristics of its core component, the parallel platform. The kinematic model of a parallel platform not only involves its geometric structural parameters, but is also closely related to the adjustment of the platform's pose, ensuring the stability and uniformity of forces during the polishing process. To accurately describe the motion state of the parallel platform, two coordinate systems are established: an FCS and a dynamic coordinate system (DCS), as shown in Figure 2.

In Figure 2, vertices A, B, C and bottom points a, b, c represent the upper and lower connection points of the parallel platform, respectively. Two coordinate systems are marked in the figure, namely the FCS OXYZ and the DCS oxyz, which are connected by three scalable branch circuits controlled by three actuators. To simplify the computational complexity of the model and enhance the efficiency of real-time control response, the following assumptions are made in the study: The rotation of the moving plate mainly revolves around a fixed axis, and the translational motion mainly occurs in the vertical direction. This simplification is based on the kinematic decoupling design principle of parallel mechanisms. Through the optimization of structural parameters, partial decoupling of rotational and translational motions is achieved, which can reduce the difficulty of trajectory planning and the complexity of control algorithms. At the same time, considering the actual working conditions of most casting grinding scenarios, which mainly feature planar and shallow curved surfaces and have vertical direction attitude adjustment as the core requirement, it can meet the precision requirements of conventional grinding tasks. For the grinding of castings with features such as deep cavities and complex free-form surfaces, this simplification has limitations. Constant force grinding requires the tool posture to conform to the normal changes of the workpiece surface in real time. The parallel mechanism with limited degrees of freedom is prone to cause normal tracking deviation, affecting the uniformity of grinding quality. For the grinding requirements of complex castings, the adaptability to complex surfaces can be further enhanced by increasing the degree of freedom of the side chain drive, introducing a multi-axis attitude cooperative control algorithm to optimize the model, and combining the contact force information fed back by the force sensor to correct the trajectory in real time. The simplification of the rotation matrix is shown in Equation 4.

$$\mathbf{R}(\theta) = \begin{bmatrix} \cos\theta & -\sin\theta & 0 \\ \sin\theta & \cos\theta & 0 \\ 0 & 0 & 1 \end{bmatrix} \tag{4}$$

In Equation 4, $\mathbf{R}(\theta)$ denotes the rotation matrix that describes the rotation state of the moving plate, and θ is the rotation angle of the moving plate around the Z-axis. This simplified model can effectively describe the main motion characteristics of the moving plate during the polishing process, while reducing the complexity of the model and facilitating subsequent kinematic analysis and control strategy design. The mapping relationship between the speed of branch extension and the speed of the moving plate is shown in Equation 5.

$$\overline{L_i} = \mathrm{J}_i \cdot \mathrm{V}_p \tag{5}$$

In Equation 5, $\overline{L_i}$ represents the stretching speed, J_i represents the Jacobian matrix, and V_p represents the generalized velocity vector of the moving plate. The inverse formula for the acceleration of the moving plate based on the branch acceleration is shown in Equation 6.

$$\ddot{\mathrm{X}}_p = \mathrm{J}^{-1}\ddot{\mathrm{L}} - \dot{\mathrm{J}}\mathrm{V}_p \tag{6}$$

In Equation 6, $\ddot{\mathrm{X}}_p$ is the generalized acceleration vector of the moving plate, $\ddot{\mathrm{L}}$ is the branch extension acceleration vector, and $\dot{\mathrm{J}}$ denotes the time derivative of the Jacobian matrix. The kinematic model of the CFPD for castings is denoted in Figure 3.

In Figure 3, the kinematic model of the CFPD for castings consists of a static plate and a dynamic plate. The static plate is fixed and equipped with a static coordinate system, while the dynamic plate is movable and equipped with a DCS. The two are connected by three extendable branches. The hinge points A, B, and C on the static plate are connected to the hinge points a, b, and c on the dynamic plate, respectively, to each branch. The inverse kinematics module calculates the lengths L1, L2, and L3 of each branch based on the expected pose of the moving plate. The control system adjusts the pose of the moving plate based on these lengths to adapt to the surface of the casting. At the same time, the sensor feeds back the polishing force data for real-time correction by the system to ensure that the polishing force is constant. The polishing tool is installed on the moving plate to perform the actual polishing task.

2.3 Control strategy of constant force polishing device for castings based on PLC

After establishing the kinematic model of the CFPD for castings, the research shifted to the design of a PLC-based control system to achieve automated operation and precise control of the device. PLC is selected as the core of the control system due to its high reliability, ease of programming, and powerful processing capabilities. The PLC control system adjusts the position and speed of the polishing head based on preset control algorithms by receiving real-time data from force sensors. The control algorithm adopts PID control strategy, in which the proportional, integral, and derivative parameters are adjusted according to the polishing requirements (Vosniakos et al., 2022; Wellendorf et al., 2023). The research adopts a control system based on PLC, which brings the characteristics of high reliability, convenient programmability and strong anti-interference ability in industrial environment to the controller design. It can stably receive real-time data from the force sensor and efficiently execute the PID control algorithm, meeting the requirements of continuous operation and complex working conditions in the casting polishing process. If the switch is made to a microcontroller-based solution, the control law needs to be adjusted at the hardware resource adaptation level. For instance, in response to the storage and computing capacity limitations of the microcontroller, the real-time reasoning process of the 49 fuzzy rules in the fuzzy PID can be simplified, or a segmented parameter update strategy can be adopted to replace the continuous adaptive adjustment with a 50 ms cycle in the original PLC system. At the same time, additional peripheral circuits need to be designed to make up for the deficiencies of the microcontroller in industrial-grade signal acquisition and drive output stability, ensuring that the control accuracy and response speed meet the polishing requirements.

Aiming at the traditional PID control strategy, an improved control method has been proposed to enhance the control accuracy and response speed of the CFPD for castings. The improved PID control strategy introduces fuzzy logic and adaptive mechanism on the basis of the original PID controller to better adapt to the uncertainty and nonlinear characteristics in the polishing process. The improved PID control strategy is denoted in Figure 4.

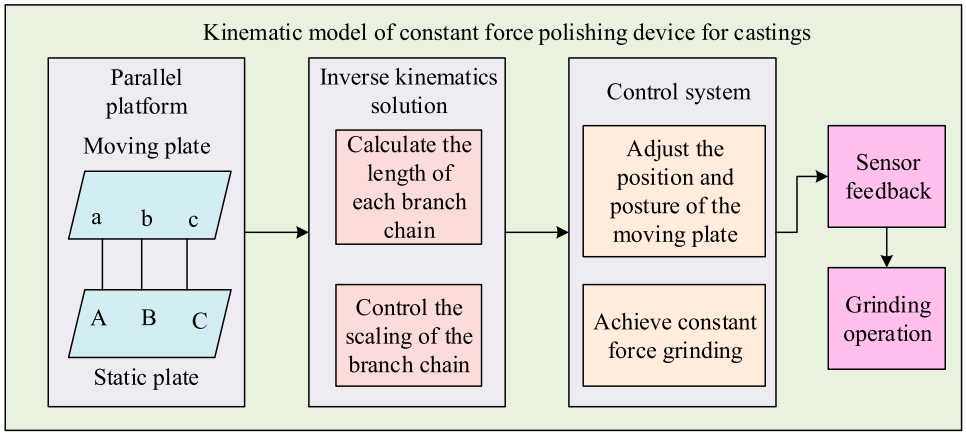

FIGURE 3
Kinematic model of constant force polishing device for castings.

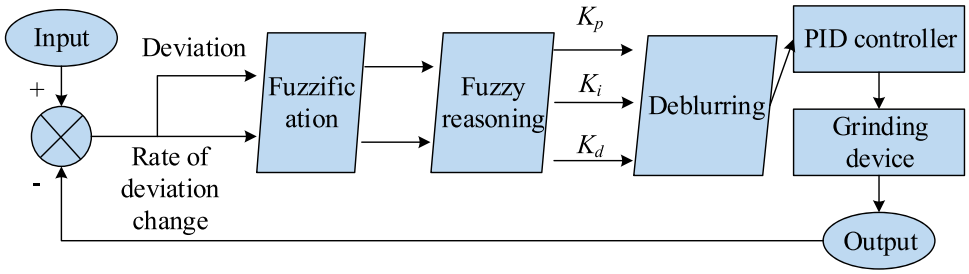

FIGURE 4
Improved PID control strategy.

In the improved PID control strategy, the fuzzy controller takes the grinding contact force error and the error change rate as inputs. The actual value ranges of the two are respectively set as −5 N–5 N and −2 N/s to 2 N/s, and are converted to the fuzzy value range of −3 to 3 through quantization factors. The fuzzy values are all classified into seven levels: “negative large, negative medium, negative small, zero, positive small, medium, and large”. The membership functions adopt triangular functions to balance accuracy and computational efficiency. Based on the grinding process experience, a fuzzy rule base containing 49 rules is constructed. The 49 fuzzy rules are constructed based on the process requirements and control logic of constant force polishing of castings. Firstly, the actual ranges of the two input variables of the fuzzy controller, namely the polishing contact force error and the error change rate, are respectively set as -5N–5 N and -2 N/s to 2 N/s, and are transformed into a fuzzy domain of −3 to 3 through quantization factors. All of them are divided into seven fuzzy subsets: “negative large, negative medium, negative small, zero, positive small, medium, and large”, and the output variables are the proportional parameter correction, integral parameter correction, and differential parameter correction for PID control. Since each of the two input variables contains 7 fuzzy subsets, a total of 49 full coverage rules of 7 × 7 are ultimately formed. The rule is presented in the form of a conditional statement: “If the contact force error is a certain fuzzy subset and the rate of error change is a certain fuzzy subset, then the proportional parameter correction, integral parameter correction, and differential parameter correction are respectively the corresponding fuzzy subsets.” When the contact force error is zero and the rate of error change is also zero, the rule is “If the contact force error is zero and the rate of error change is zero, then the correction amount of the proportional parameter is zero, the correction amount of the integral parameter is positive, and the correction amount of the differential parameter is zero”, so as to maintain the stability of the proportional parameter and fine-tune the integral effect to eliminate the steady-state error. After all the rules are processed through reasoning and weighted average defuzzification, the actual correction values are output to achieve dynamic adjustment of PID parameters.

The correction values of the proportional coefficient, integral coefficient and differential coefficient are output through the Mamdani reasoning method and the weighted average anti-fuzzification method, and then converted into actual adjustment values by the scaling factor. The adaptive mechanism takes 50 ms as one control cycle, collects feedback data from the force sensor in real time, and calculates the error integral value and the error square integral value within each cycle. When the error integral value is greater than 0.5 N·s for three consecutive cycles, or the error square integral value

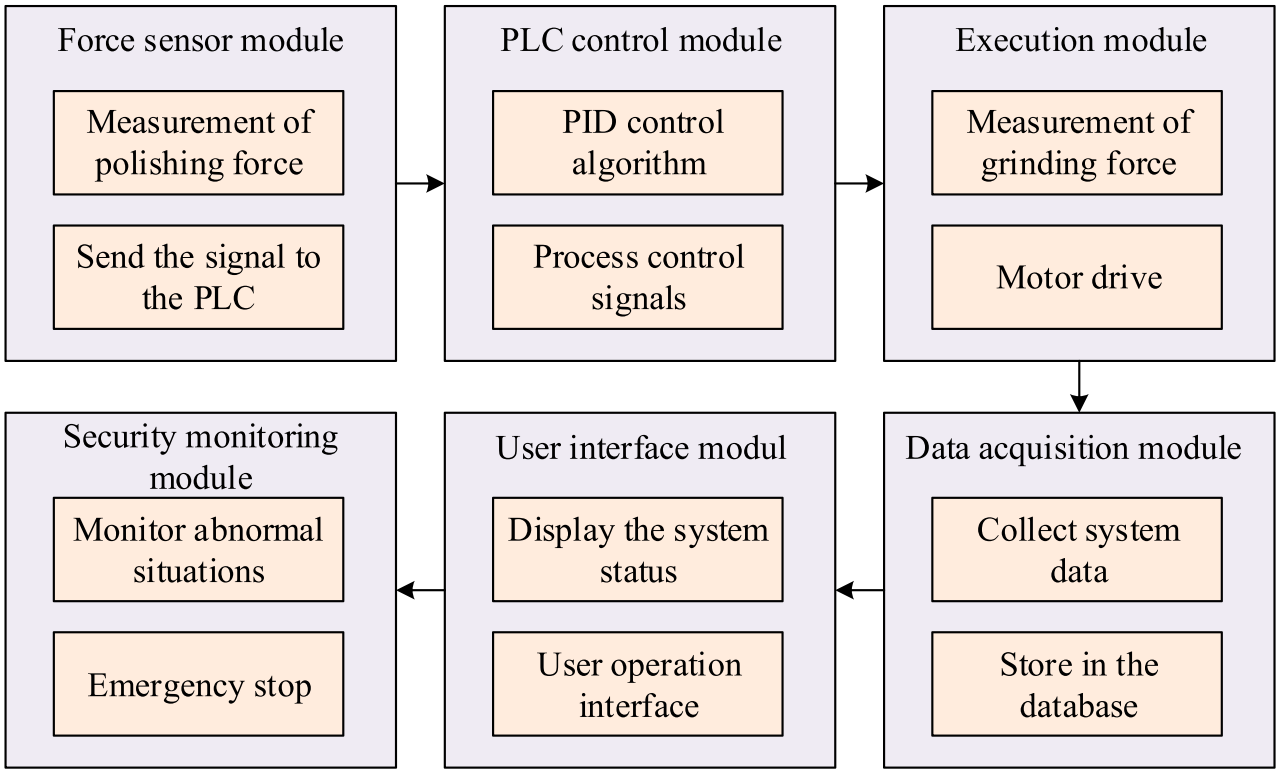

FIGURE 5
System architecture diagram of constant force polishing device for castings.

suddenly changes by more than 20%, it is determined that the dynamic characteristics of the system have changed. Immediately trigger the update of the parameter reference value. The recursive least square method is adopted to fit the optimal parameter sequence of the first 100 cycles, establish the corresponding relationship between the proportional coefficient, integral coefficient, differential coefficient and the error characteristic quantity, update the initial parameter reference value of the fuzzy controller to adapt to the new working conditions, and achieve the adaptive integration of static fuzzy rules and dynamic parameters. The improved PID control strategy is shown in Equation 7.

$$u(t) = f\left(K_p, K_i, K_d, e(t), \dot{e}(t), \ddot{e}(t)\right) \tag{7}$$

In Equation 7, $u(t)$ is the control input, $e(t)$ is the error, $\dot{e}(t)$ is the rate of change of the error, $\ddot{e}(t)$ is the rate of change of the error rate, and f is a nonlinear function that adjusts PID parameters based on fuzzy logic and adaptive algorithms. The position error between the actual polishing trajectory and the expected trajectory is shown in Equation 8.

$$e_{\text{pos}} = \sqrt{(x_d - x_a)^2 + (y_d - y_a)^2 + (z_d - z_a)^2} \tag{8}$$

In Equation 8, (x_d, y_d, z_d) represents the expected trajectory coordinates, (x_a, y_a, z_a) represents the actual trajectory coordinates, and e_{pos} represents the position error. To accurately quantify the polishing deviation, an error calculation model is constructed as denoted in Equation 9.

$$e_{pos}(t) = r_d(t) - r_a(t) \tag{9}$$

In Equation 9, $e_{pos}(t)$ denotes the position error vector at time t, $r_d(t)$ refers to the position vector of the expected polishing trajectory, and $r_a(t)$ refers to the position vector of the actual polishing trajectory. The system architecture of the CFPD for castings is shown in Figure 5.

In Figure 5, the CFPD system for castings is an integrated control and execution system, in which the force sensor module is responsible for real-time measurement and feedback of polishing force, the PLC control module uses PID algorithm to process sensor data and generate control instructions, and the execution module is composed of a motor and a sand wheel, which actually performs polishing tasks. The data collection module is responsible for collecting and storing system operation data. The user interface module provides human-computer interaction, displays system status, and receives user instructions. The security monitoring module ensures the safe operation of the system, monitors anomalies, and triggers emergency stops when necessary. The research adopts an automated polishing method based on a parallel platform, with a customized parallel mechanism as the core execution unit. The grinding tool is mounted at the end of the moving platform of the parallel platform, and the pose control of the end effector is achieved by establishing a kinematic model. Its control strategy focuses on the constant force grinding requirements and innovatively introduces an improved PID control method that integrates fuzzy logic and adaptive mechanisms. The grinding

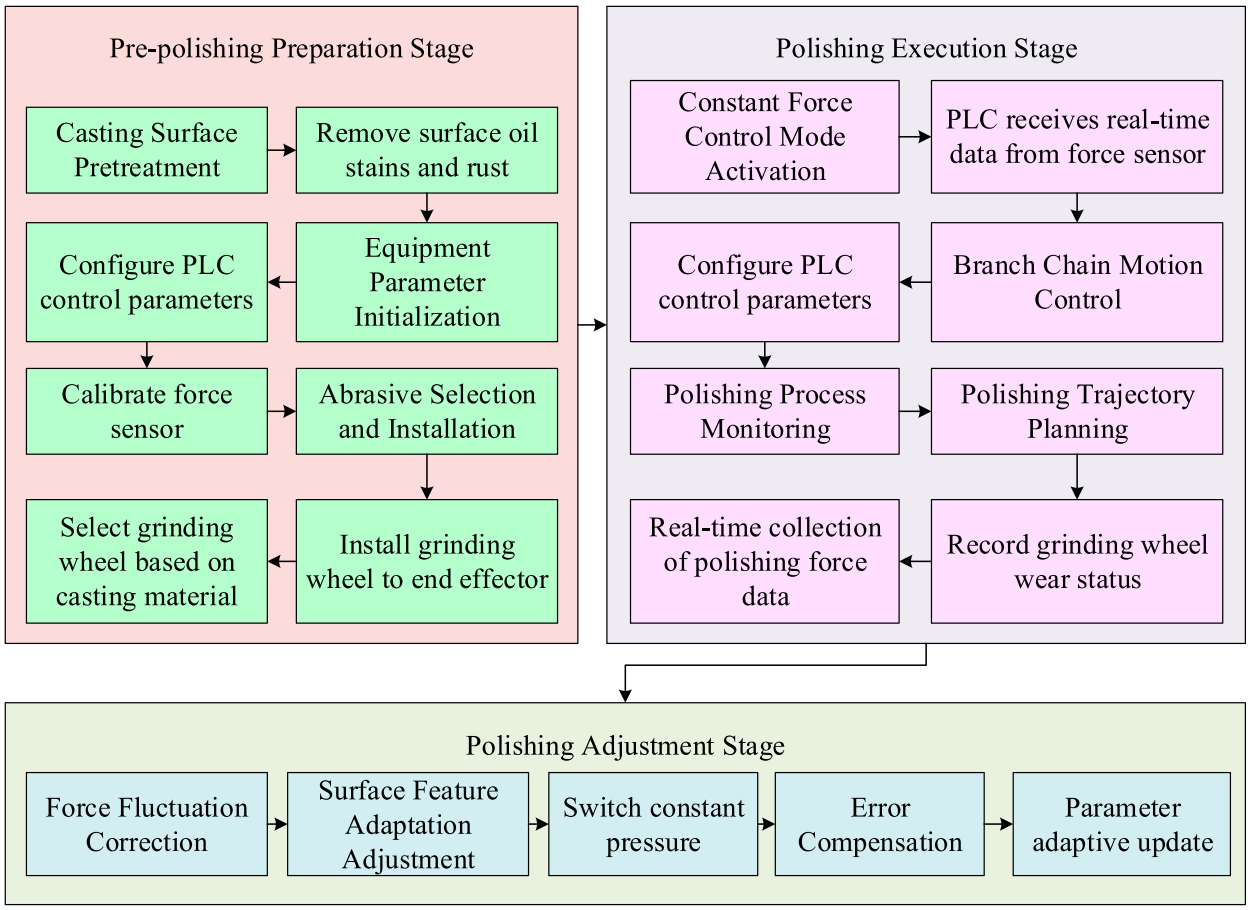

FIGURE 6
Polishing method of constant force polishing device for casting.

contact force signal is collected in real time through the force sensor. The error and the rate of error change are processed by the fuzzy controller to dynamically correct the PID parameters. Then, combined with the adaptive mechanism, the parameter reference values are updated according to the changes in system characteristics. Eventually, the dual control of the trajectory accuracy of the end actuator and the stability of the contact force is achieved, which is suitable for the polishing requirements of low-complexity surfaces in castings. It makes up for the defect of traditional position control that is prone to fluctuations in grinding quality due to workpiece errors. In the actual polishing process, the change in the contact area between the polishing head and the workpiece will affect the uniformity of the polishing effect. The research adopts a constant pressure - constant force compound control strategy. By integrating a micro pressure sensor array at the end of the polishing head, the pressure distribution in the contact area is monitored in real time. When the local pressure deviation exceeds the preset threshold, it automatically switches to the constant pressure control mode. The change in contact area is dynamically compensated by adjusting the feed rate of the parallel platform to keep the pressure per unit area constant. After the contact state stabilizes, switch back to the constant force control to ensure the overall polishing efficiency. The polishing method of the constant force polishing device for castings based on kinematic analysis is shown in Figure 6.

In Figure 6, the preparation stage focuses on the pretreatment of castings, the initialization of equipment parameters and the installation of grinding tools, clarifying key details such as the calibration of force sensors and the calculation of grinding wheel linear velocity. The execution stage takes constant force control as the core, correlating the PLC control algorithm, the kinematic model of the parallel platform and the trajectory planning logic, and reflecting the adaptation strategies for different surface features. In the adjustment stage, a dynamic correction scheme is designed for force fluctuations, surface feature changes and position errors, and the parameter adjustment rules of the improved PID are integrated.

3 Results and analyses

The performance of the CFPD for castings was comprehensively verified and analyzed in the results section of the study. Through motion simulation and adaptability verification, the polishing trajectory accuracy, polishing force stability, adaptability, and response time of the device under different surface characteristics

TABLE 2 Simulation configuration and parameters.

Parameter name	Parameter description	Value
Software model	The name and version of the simulation software	ADAMS 2022
Parallel platform model	The model and specification of the parallel platform mechanism	LPS-300–600
Fixed plate size	The physical dimensions of the fixed plate	600 mm × 400 mm
Moving plate size	The physical dimensions of the moving plate	500 mm × 300 mm
Side chain length	The length of the side chain in its initial state	700 mm
Actuator model	The model of the electric actuator driving the branch chain	BLAC100

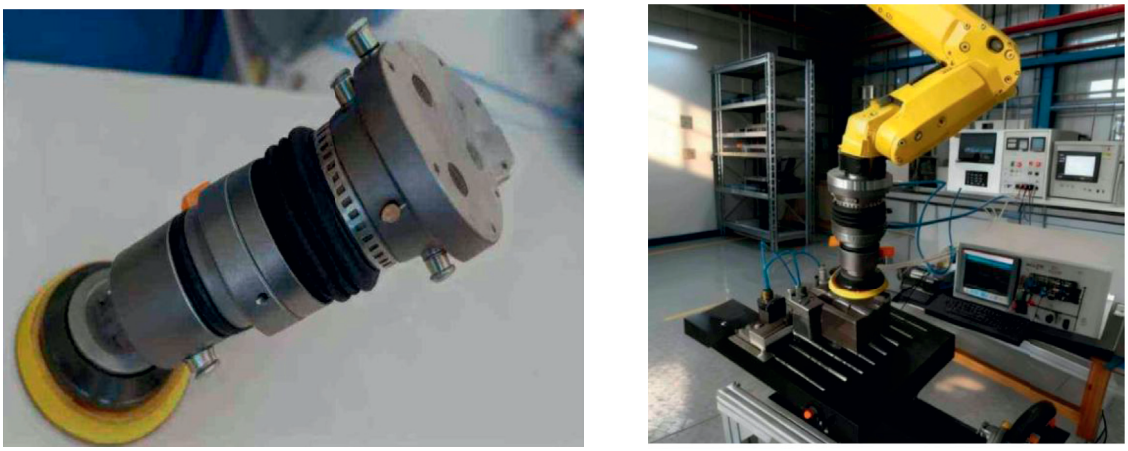

FIGURE 7
Polishing device and experimental platform. **(a)** Polishing device. **(b)** Experimental platform.

of castings were studied and evaluated. The PLC-based control system was validated, and the application effects of different control algorithms in the polishing process were compared, thus comprehensively demonstrating the actual operational performance of the CFPD for castings.

3.1 Motion simulation and adaptability verification of constant force polishing device for castings

When conducting motion simulation and adaptability verification of the CFPD for castings, simulation software Advanced Dynamics and Multibody Software (ADAMS) was used in the study. To verify the adaptability of the device, a dataset was created that includes various typical surface features of castings, including planes, surfaces, irregular protrusions, and depressions. The dataset provides detailed records of the geometric parameters and expected polishing force values for each surface feature. The simulation configuration and parameters are denoted in Table 2.

In Table 2, the simulation configuration included a three degree of freedom parallel platform mechanism that simulates an actual polishing device. The parallel platform used in the simulation has the following technical parameters: the upper fixed plate size was 600 mm × 400 mm, the lower floating plate size was 500 mm × 300 mm, the initial length of the branch was set to 700 mm, and the branch was driven by an electric actuator model BLAC100, which has high torque and precise positioning capability. The polishing device and the experimental platform are shown in Figure 7.

Figure 7a shows the polishing device, equipped with a flexible buffer structure in the middle, which can adapt to the pressure changes during the polishing process. The bottom polishing pad is an actuating component that directly acts on the surface of the workpiece. Figure 7b shows the experimental platform. The end of the mechanical arm is connected to the polishing device, and the fixture below holds the workpiece to be processed. Control devices and data acquisition instruments are equipped beside the platform. The polishing trajectory accuracy under different surface features is shown in Figure 8. The calculation of trajectory accuracy takes the spatial position deviation between the actual grinding trajectory and the expected trajectory as the core measurement: Firstly, the actual coordinate sequence of the end effector during the grinding process is obtained through a laser displacement sensor and matched point by point with the preset expected grinding trajectory coordinate

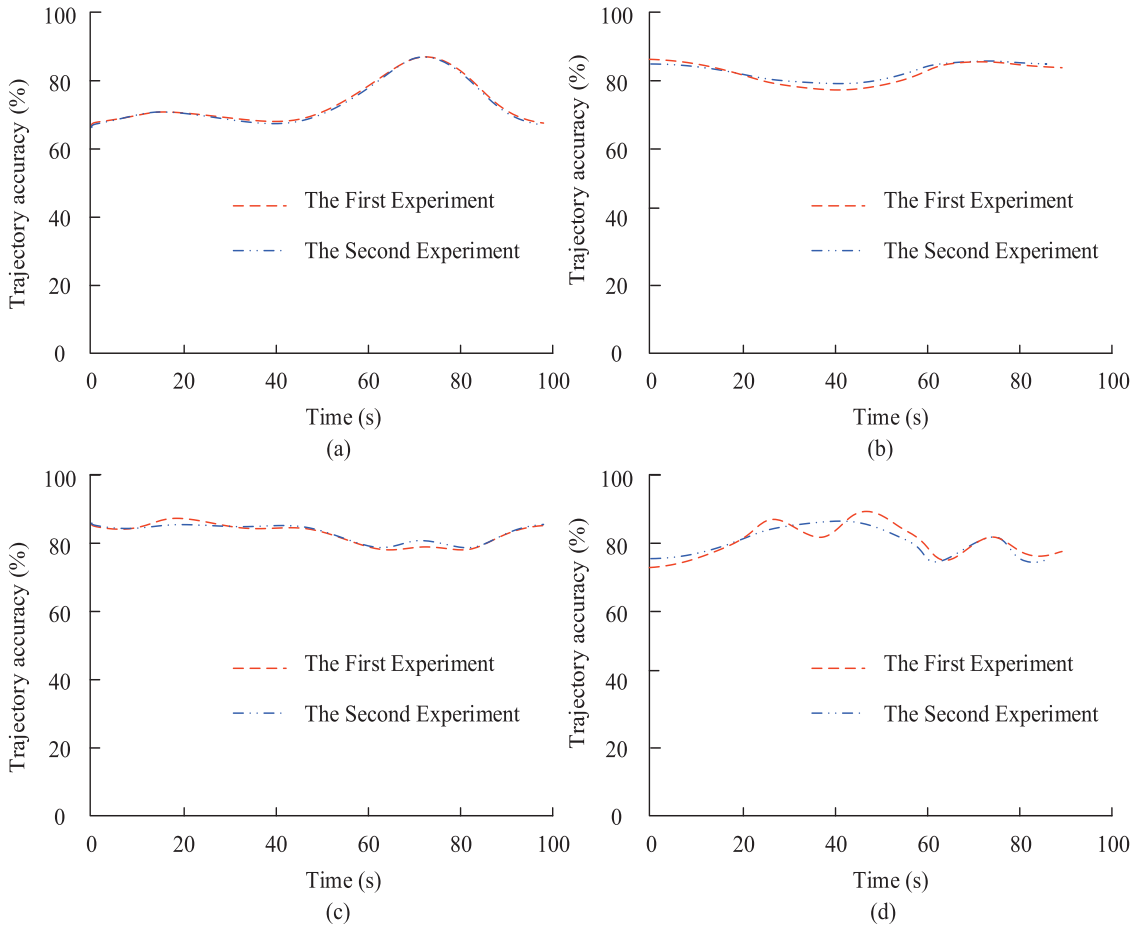

FIGURE 8
Comparison of polishing trajectory accuracy under different surface features. **(a)** Planar feature trajectory accuracy. **(b)** Surface feature trajectory accuracy. **(c)** Irregular raised trajectory accuracy. **(d)** Depression feature trajectory accuracy.

sequence. Secondly, calculate the Euclidean distance of each pair of matching points in three-dimensional space, and statistically calculate the arithmetic mean of the pose deviations of all single points. Finally, (1 - average deviation/total expected trajectory length) × 100% is taken as the final quantification result of trajectory accuracy, with the total expected trajectory length being the spatial curve length of the preset grinding path.

In Figure 8a, the trajectory accuracy gradually increased from 65% to nearly 90% when polishing planar features. It showed good adaptability and stability during the polishing process, especially in the latter half of the time when the trajectory accuracy was significantly improved. In Figure 8b, during the surface feature polishing process, the trajectory accuracy of both experiments remained above 80%. In Figure 8c, for the polishing of irregular convex features, the trajectory accuracy of Experiment 1 and Experiment 2 experienced a trend of first decreasing and then increasing, finally stabilizing between 80% and 90%, indicating good adaptability to irregular features. In Figure 8d, the trajectory accuracy of the concave feature polishing fluctuated between 70% and 90% in both experiments. Under different surface characteristics of castings, the polishing trajectory accuracy of the two experiments meets the expected working requirements. The stability of polishing force under different surface features is shown in Figure 9.

In Figure 9a, in the first experiment, the average polishing force of planar features remained stable between approximately 490 and 500 N, while the average polishing force of irregular convex features gradually increased from 510 N to around 520 N and remained stable. The average polishing force of the surface features remained around 540 N with minimal fluctuations, demonstrating extremely high stability. The average polishing force of concave features started from 550 N, slightly decreased and stabilized between 540 N and 560 N. In Figure 9b, the average polishing force of the planar features remained stable between 490 and 500 N throughout the entire experimental process. The average polishing force of irregular convex features started from 510 N, gradually increased to around 520 N, and remained stable. The average polishing force of concave features started from 550 N, slightly decreased and stabilized between 540 N and 560 N. The adaptability and response time of polishing under different surface features are shown in Figure 10.

In Figure 10a, for irregular convex features, the adaptability started from about 90%, slightly decreased, and finally stabilized at

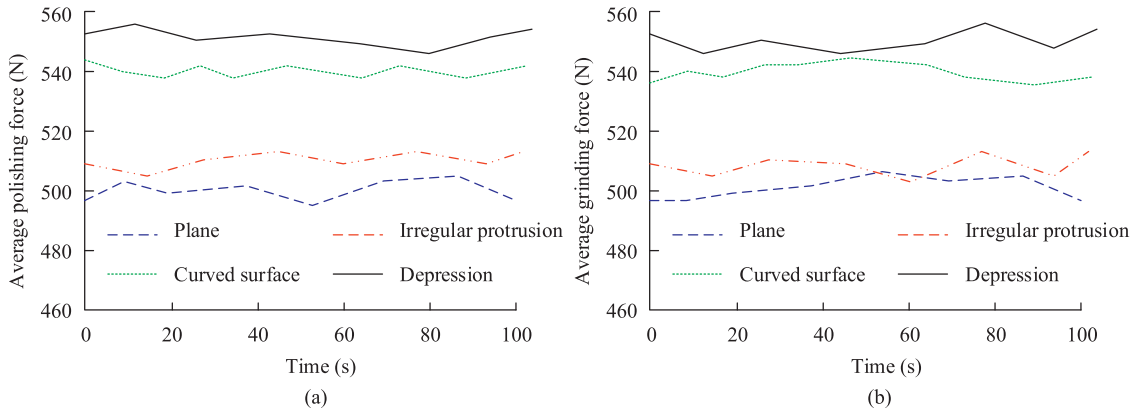

FIGURE 9
Comparison of stability of polishing force under different surface features. **(a)** The first experiment. **(b)** The second experiment.

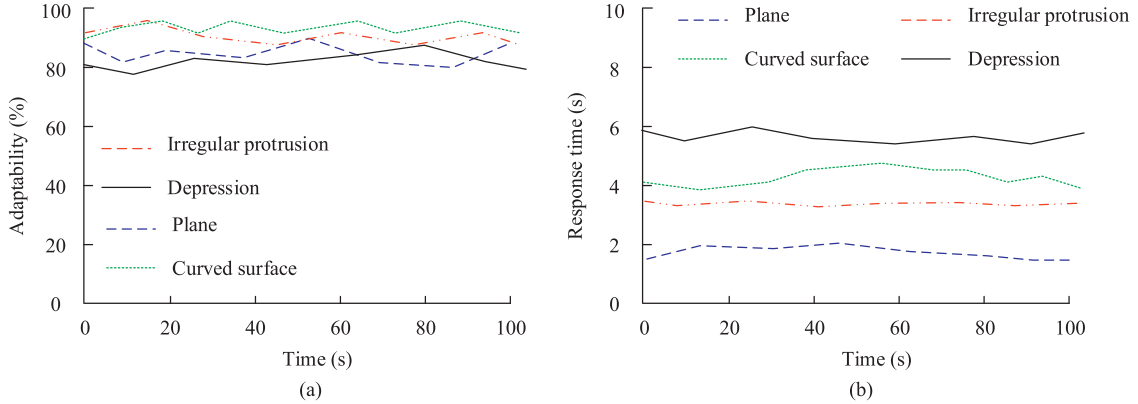

FIGURE 10
Comparison of adaptability and response time of polishing under different surface features. **(a)** Adaptability. **(b)** Response time.

around 85%. For planar features, adaptability started at 80% and gradually increased to 85%, indicating an improvement in adaptability to planar features over time. In Figure 10b, the response time of the irregular convex feature remained at approximately 3.50 s, indicating a faster response speed. The response time of the concave feature started from 6.00 s and gradually decreased to 5.50 s. Although the response time was initially longer, it eventually showed an improvement in response speed.

3.2 Verification of control system for constant force polishing device for castings

The research verified the control system of the CFPD for castings. Firstly, the research tested the performance of the improved PID control algorithm by comparing traditional PID control algorithm, improved PID control algorithm, Fuzzy Control (FC) algorithm, and Adaptive Control (AC) algorithm. The parameter Settings and control law forms of each control algorithm are as follows: The PID control algorithm adopts a proportional coefficient of 0.8, an integral coefficient of 0.05, and a differential coefficient of 0.2. The control law is the linear superposition of the deviation and the proportional term, integral term, and differential term. The improved PID control algorithm introduces an error piecewise adjustment mechanism on its basis. When the absolute value of the error is greater than 2 N, the proportional coefficient increases to 1.0 and the differential coefficient is adjusted to 0.3. When the absolute value of the error is ≤2 N, the integral coefficient increases to 0.08. The control law is a nonlinear piecewise weighted combination. The FC algorithm sets the error domain [-5,5] and the error change rate domain [-2,2], containing 49 fuzzy rules. The control law is to output the control quantity through fuzzy reasoning. The AC algorithm adopts a model reference adaptive structure. The parameter adaptive law is that the proportional gain is positively correlated with the square integral of the error. The control law is to correct the control quantity in real time to track the output of the reference model. The motion simulation is the verification result of the ADAMS simulation environment. This simulation builds the control algorithm test scenario based on the parameters such as the parallel platform model (LPS-300–600) and the electric actuator

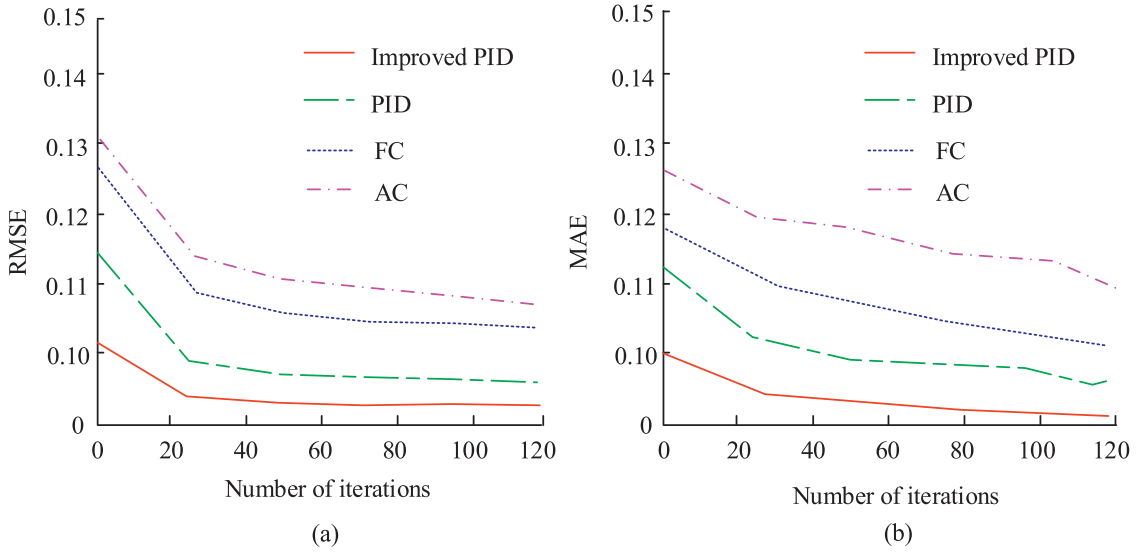

FIGURE 11
Comparison of RMSE and MAE for several control algorithms. **(a)** RMSE. **(b)** MAE.

TABLE 3 Application effect of different control algorithms in constant force polishing device for castings.

Performance indicators	PID	FC	AC	The control system designed by the research
Anti-interference ability	6.50	7.10	7.90	8.40
Stability index	0.13	0.11	0.10	0.09
Error recovery time (s)	5.50	4.80	4.50	4.00
RMSE (%)	2.30	1.90	1.70	1.60
Maximum error (%)	6.00	5.50	5.00	4.50
Response time (s)	11.00	9.50	8.50	7.50
Steady-state error	0.50	0.40	0.35	0.30
Overshoot	8.00	6.00	4.00	3.00
Frequency response	0.80	0.85	0.90	0.95
Robustness	0.75	0.85	0.88	0.90

(BLAC100) set in Table 2. The Root Mean Square Error (RMSE) and Mean Absolute Error (MAE) of several control algorithms are shown in Figure 11.

In Figure 11a, the RMSE starting value of the improved PID algorithm was the lowest, about 0.10, and then rapidly decreased. After about 20 iterations, it tended to stabilize and eventually stabilized at around 0.08. The improved PID algorithm performed the best in reducing RMSE, achieving a steady state faster and with the lowest error value. In Figure 11b, the initial MAE of the improved PID algorithm was the lowest, about 0.10, rapidly decreasing and stabilizing at around 0.07 after approximately 20 iterations. This further confirmed the advantages of the improved PID algorithm in reducing MAE, with the lowest error value and the fastest stable speed. To evaluate the practical application effect of different control algorithms in the CFPD for castings, the study compared traditional PID control, FC, AC, and the control system designed by the research. The application performance of different control algorithms in the CFPD for castings are denoted in Table 3.

In Table 3, the control system designed for the study scored 8.40 in terms of anti-interference ability, significantly higher than other algorithms, demonstrating stronger resistance to external disturbances. In terms of error recovery time, the system only took 4.00 s, which was much faster than other algorithms, indicating its ability to adjust and recover errors very quickly. The RMSE of the control system designed for research was1.60, with a maximum error of 4.50%, which was the lowest value among all algorithms, further confirming its high-precision characteristics. The response time was also the fastest, only 7.50 s, indicating that the system can quickly respond to changes during the polishing process.

In the verification of polishing trajectory accuracy, the accuracy of planar feature polishing trajectories has gradually increased from 65% to nearly 90%, the accuracy of curved surface feature trajectories has remained stable at over 80%, and the accuracy of irregular protruding and concave feature trajectories has stabilized at 70%–90% after fluctuation, demonstrating the device's trajectory adaptation ability to different surfaces. In the verification of the stability of polishing force, the average polishing force of the planar features remained stable at 490 N–500 N, while the average polishing forces of other features remained stable with minimal fluctuations after minor adjustments, reflecting the adaptability of force control of the device during processing on different surfaces. In the verification of adaptability and response time, the adaptability of planar features increased from 80% to 85%, the adaptability of irregular protruding features remained stable at around 85%, the response time of irregular protruding features stabilized at 3.50 s, and the response time of concave features decreased from 6.00 s to 5.50 s, further confirming the dynamic adaptation effect of the device to different surface features.

4 Conclusion and future works

The research aimed to design a CFPD that can meet the high-precision and high-efficiency machining requirements of large castings. The structure design and optimization of the CFPD for castings were carried out using kinematic analysis methods, and a kinematic model was established. At the same time, a PLC-based control system was constructed, and an improved PID control strategy was introduced to achieve automation and precise control of the polishing process. The research results showed that in motion simulation and adaptability verification, the trajectory accuracy of the designed device could reach 88% when polishing planar features, and remained stable at over 85% when polishing curved features. For polishing irregular protrusions and depressions, the trajectory accuracy could also be maintained between 75% and 90%. The improved PID control strategy significantly improved control accuracy and response speed. Its RMSE stabilized at around 0.07 after 20 iterations, MAE stabilized at around 0.06, and error recovery time was only 4.0 s, far superior to traditional PID control and other algorithms. A kinematic analysis-based CFPD for castings has been successfully designed and validated, which performs well in high-precision force control and adaptability to complex surface characteristics of castings. At present, the performance verification of the constant force grinding device for castings is all carried out based on the ADAMS simulation software. Although the simulation results have demonstrated the excellent performance of the device in terms of trajectory accuracy, force stability and control response, in order to further enhance the industrial application persuasiveness of the results, physical experiments need to be conducted for verification in subsequent research. At the same time, in response to possible problems such as branch chain vibration and force feedback delay in the experiment, the structural damping design and control algorithm parameters were optimized to further enhance the industrial applicability of the device.

Data availability statement

The original contributions presented in the study are included in the article/supplementary material, further inquiries can be directed to the corresponding author.

Author contributions

FZ: Writing – original draft, Writing – review and editing.

Funding

The author(s) declared that financial support was not received for this work and/or its publication.

Conflict of interest

The author(s) declared that this work was conducted in the absence of any commercial or financial relationships that could be construed as a potential conflict of interest.

Generative AI statement

The author(s) declared that generative AI was not used in the creation of this manuscript.

Any alternative text (alt text) provided alongside figures in this article has been generated by Frontiers with the support of artificial intelligence and reasonable efforts have been made to ensure accuracy, including review by the authors wherever possible. If you identify any issues, please contact us.

Publisher's note

References

Buonocore, S., Di Gironimo, G., Favaretto, M., Grasso, T., Zanon, F., and Grazioso, S. (2023). Systems engineering approach for the iterative concept design and virtual simulation of the DTT hyper redundant manipulator. *Fusion Eng. Des.* 190 (5), 113534.1–113534.11. doi:10.1016/j.fusengdes.2023.113534

Emet, H., Guer, B., and Dede, M. S. C. (2024). The design and kinematic representation of a soft robot in a simulation environment. *Robotica Int. J. Inf. Educ. Res. Robotics Artif. Intell.* 42 (1), 139–152. doi:10.1017/S026357472300139X

Lyu, Z., and Purwar, A. (2025). Point-based models: a unified approach for geometric constraint analysis of planar n -bar mechanisms with rotary, sliding, and rolling joints. *J. Mech. Robotics* 17 (4), 1–8. doi:10.1115/1.4066963

Pacioni, S., Carbonari, L., Martarelli, M., and Callegari, M. (2024). Design and simulation of a desk-size parallel kinematic machine for simulation of seismic events. *Meccanica* 59 (12), 2313–2323. doi:10.1007/s11012-024-01911-1

Ramanababu, S., and Ramji, K. (2024). Kinematic analysis and design optimization of 2UPR-2RPU redundant parallel manipulator. *Trans. Indian Natl. Acad. Eng.* 9 (2), 375–383. doi:10.1007/s41403-024-00459-6

Scavalla, A., Rossi, A., Battaglia, V. L., and Belfiore, N. (2023). A survey of wave energy converter mechanisms presented under the topological and functional viewpoints. *J. Mech. Des.* 145 (7), 070801–070820. doi:10.1115/1.4057057

Simas, H., Di Gregorio, R., and Simoni, R. (2022). TetraFLEX: design and kinematic analysis of a novel self-aligning family of 3T1R parallel manipulators. *J. Field Robotics* 39 (5), 617–630. doi:10.1002/rob.22067

Song, Z., Li, X., Yang, X., Li, Y., Wang, L., and Wu, H. (2023a). Kinematic modeling of a spatial three degrees-of-freedom compliant micro-motion parallel mechanism considering input coupling effect and bilateral restrained torsion. *Ind. Robot.* 50 (3), 385–400. doi:10.1108/IR-06-2022-0146

Song, J., Wei, J., Yu, B., Liu, C., Ai, C., and Zhang, J. (2023b). Configuration design and kinematic performance analysis of a novel 4-DOF parallel ankle rehabilitation mechanism with two virtual motion centers. *Chin. J. Mech. Eng.* 36 (6), 87–104. doi:10.1186/s10033-023-00977-4

Song, M., Li, Z., Jiang, J., Chen, W., Guo, S., Zheng, H., et al. (2024). Design, simulation and kinematic validation of a hip prosthetic mechanism with a multimotor function. *J. Bionic Eng.* 21 (3), 1321–1333. doi:10.1007/s42235-024-00490-x

Sun, Z., Li, Y., Zi, B., and Chen, B. (2023). Design, modeling, and evaluation of a hybrid driven knee-ankle orthosis with shape memory alloy actuators. *J. Mech. Des.* 145 (6), 063301–063313. doi:10.1115/1.4056692

Trojnacki, M., and Dabek, P. (2024). Simulation research of motion of lightweight wheeled mobile robot on various types of soft ground - a case study. *J. Automation, Mob. Robotics Intelligent Syst.* 17 (4), 8–16. doi:10.14313/jamris/4-2023/26

Vosniakos, G. C., Katsaros, P., Papagiannoulis, I., and Meristoudi, E. (2022). Development of robotic welding stations for pressure vessels: interactive digital manufacturing approaches. *IJIDeM Int. J. Interact. Des. Manuf.* 16 (1), 151–166. doi:10.1007/s12008-021-00813-w

Wang, C., Wang, Z., and Hu, H. L. L. (2023). Innovative design and kinematic characteristics analysis of floating mobile chassis of inspection robot. *Machines* 11 (1), 1–22. doi:10.3390/machines11010024

Wei, M. Y. (2022). Design of a DSP-based motion-cueing algorithm using the kinematic solution for the 6-DoF motion platform. *Aerosp.* 9 (4), 1–25. doi:10.3390/aerospace9040203

Wei, F., Luo, K., Zhang, Y. J. J., and Jiang, J. (2024). Structural design and kinematic analysis of cable-driven soft robot. *Actuators* 13 (12), 1–19. doi:10.3390/act13120497

Wellendorf, A., Tichelmann, P., and Uhl, J. (2023). Performance analysis of a dynamic test bench based on a linear direct drive. *Archives Adv. Eng. Sci.* 1 (1), 55–62. doi:10.47852/bonviewAAES3202902

Xu, H., Wang, L., Miao, Y. S. L., and Sun, L. (2024). Kinematic synthesis and optimization design of a rice pot seedling transplanting mechanism. Proceedings of the Institution of Mechanical Engineers, Part C. *J. Mech. Eng. Sci.* 238 (5), 1366–1381. doi:10.1177/09544062231184804

Yang, H., Jiang, S., and Xiao, W. H. (2023). Design, kinematic and fluid-structure interaction analysis of a morphing wing. *Aerosp. Sci. Technol.* 143 (12), 108721.1–108721.16. doi:10.1016/j.ast.2023.108721

Yitao, P., Gangfeng, L., Yuan, S. C., Wang, S., and Chen, Y. (2024). Design and kinematic analysis of the four-level rigid trunk mechanism based on 4-SPS/U. *Mech. Based Des. Struct. Mach.* 52 (1/2), 72–101. doi:10.1080/15397734.2022.2096629